



Published in final edited form as:

*Environ Sci Technol.* 2023 December 05; 57(48): 20410–20420. doi:10.1021/acs.est.3c06586.

## ***Sous Vide*-Inspired Impregnation of Amorphous Titanium (Hydr)Oxide into Carbon Block Point-of-Use Filters for Arsenic Removal from Water**

Alireza Farsad<sup>†,‡</sup>, Mariana Marcos-Hernandez<sup>†</sup>, Shahnawaz Sinha<sup>†,‡</sup>, Paul Westerhoff<sup>†,‡,\*</sup>

<sup>†</sup>School of Sustainable Engineering and the Built Environment, Arizona State University, Tempe, AZ 85287, USA

<sup>‡</sup>Engineering Research Center for Nanotechnology-Enabled Water Treatment (NEWT), Arizona State University, Tempe, AZ 85287, USA

### **Abstract**

Carbon block filters, commonly employed as point-of-use (POU) water treatment components, effectively eliminate pathogens, adsorb undesirable tastes, odors, and organic contaminants, all while producing no water waste. However, they lack the capability to remove arsenic. Enabling carbon block to remove arsenic could reduce its exposure risks in tap water. Inspired by *Sous vide* cooking techniques, we developed a low-energy, low-chemical method for impregnating commercially available carbon block with titanium (hydr)oxide (THO) in four steps: 1) vacuum removal of air from the carbon block, 2) impregnation with precursors in a flexible pouch, 3) sealing to prevent oxygen intrusion, and 4) heating in a water bath at 80 °C for 20 hours to eliminate exposure and reactions with air. This process achieved a uniform 13 wt.% Ti loading in the carbon block. Our modified carbon block POU efficiently removed both arsenate and arsenite from tap water matrices, containing 10 or 100 µg/L arsenic concentrations, in batch experiments or continuous flow operations. Surprisingly, THO modified carbon block removed arsenite better than arsenate. This innovative method, using 70% fewer chemicals than traditional autoclave techniques, offers a cost-effective solution to reduce exposure to arsenic and lower its overall risk in tap water.

### **Keywords**

Pollution; Carbon block; Arsenic; Titanium; Adsorption

---

\*Corresponding Author p.westerhoff@asu.edu, Phone: 480-965-2885.

Supporting information

Supporting information includes: an explanation of the calculation of the required synthesis solution volume for each method; side view and top view of the used prefabricated carbon block in this study (Figure S1); the schematic illustration of the designed POU system for continuous treatment experiments (Figure S2); photographs of the designed POU system (Figure S3); the breakthrough curves of As, Se, V, and Fe obtained from POU treatment test using unmodified carbon block with actual groundwater (Figure S4); a summary of the used iron-based media for arsenic removal reported in the literature (Table S1); chemistry of Tempe tap water matrix (Table S2); chemistry of the used actual groundwater (Table S3).

## 1. Introduction

Arsenic, a metalloid of significant concern, naturally occurs in groundwater across various regions worldwide.<sup>1</sup> Individuals who primarily rely on groundwater as their source of drinking water face a considerable risk of developing multiple cancers and neural diseases due to prolonged exposure to arsenic-contaminated drinking water.<sup>2</sup> Municipalities employ a variety of treatment practices at centralized facilities to reduce arsenic concentrations in drinking water to below the maximum contamination level (MCL) of 10 µg/L. This MCL is based upon approximately a 1 in 10,000 cancer risk assessment. Thus, even when arsenic concentrations are below 10 µg/L, the cancer risk from arsenic is not zero.<sup>3</sup> Also, prenatal and early-life exposure to arsenic in more vulnerable children, even at low concentrations, results in subsequent cognitive issues.<sup>4</sup> Therefore, as a carcinogen there is no safe threshold for arsenic in drinking water, and a further reduction in arsenic exposure would reduce health risks from drinking water. In the United States, over 60% of regions have drinking water with an arsenic concentration exceeding 1 µg/L.<sup>5</sup> Consequently, an additional barrier is desirable for removing arsenic from drinking water, with point-of-use (POU) technologies proving to be a practical option. Iron-based adsorbent media have been extensively examined in the literature, resulting in the development of various granular materials available commercially for point-of-entry (POE) applications in distribution systems, such as wellhead treatment, and in POU cartridge modules. These materials have been shown to be highly effective in removing arsenic from water.<sup>6-11</sup> Table S1 provides a comprehensive comparison of literature values for arsenic adsorption capacity of iron-based sorbents. Reported adsorption capacities span two orders of magnitude, ranging from 1 to 100 mg As/g material. Performance of these adsorbents were more efficient at lower pH levels but less effective at lower initial arsenic concentrations. Most iron-based media exhibit reduced adsorption capacities for arsenite (As(III)) when compared to equimolar levels of arsenate (As(V)). This discrepancy is primarily due to the fact that arsenate is an anionic at near-neutral pH levels typical of drinking water, while arsenite is predominantly non-ionic.<sup>12</sup> There is a pressing need to develop point-of-use (POU) systems with multifunctional capabilities, capable of removing both As(V) and As(III) species, all the while achieving other treatment objectives, such as enhancing taste and odor, or adsorbing substances like PFAS and other trace organics.<sup>13,14</sup> Such systems should be compact and designed to fit within a single small-sized treatment module, eliminating wastage and conserving water resources.

Carbon block filters are widely used in POU systems to adsorb organic contaminants (e.g., PFAS) and filter pathogens.<sup>13-15</sup> However, conventional carbon block filters are unable to remove arsenic from water. Our previous work successfully enhanced the arsenic removal capabilities of prefabricated carbon block modules by impregnating them with amorphous titanium (hydr)oxide (THO) as stable metal (hydr)oxides at environmentally relevant pH values, using sol-gel techniques.<sup>16</sup> Small cylindrical pieces were excised from the carbon block to facilitate bench-scale experiments. However, to apply this modified technology in practical water treatment applications, it is necessary to impregnate full-sized carbon block modules using an effective technique that could be scalably manufactured. Due to its highly porous nature, with many micropores and mesopores, simply soaking the carbon block

in the impregnating solution may not yield effective and homogeneous impregnation.<sup>17</sup> Moreover, trapped oxygen within the pores of the porous media hinders the easy transport of the solution through the pores. Additionally, as the sol-gel solution becomes increasingly viscous over time, it becomes impractical to impregnate the carbon block by pumping the solution through the module. Therefore, the most efficient method involves applying an immediate vacuum to a carbon block immersed in the THO synthesis solution.<sup>18</sup> By removing the trapped oxygen from the carbon block structure through vacuum application, the solution can penetrate and fill the pores simultaneously and rapidly.<sup>17</sup>

Another crucial aspect is preventing contact between the synthesis solution and air moisture after impregnation and before aging. This precaution is essential as it directly affects the hydrolysis rate of the sol-gel synthesis and the resulting gel structure.<sup>19</sup> Therefore, the synthesis should proceed within a sealed environment. Because the aging temperature is a controlling factor in sol-gel synthesis,<sup>20</sup> homogenous heat transfer is essential to have an even formation and distribution of identical THO particles throughout the thickness (~1.3 cm) of the carbon block from its outer surface to the center core. Given the intricate network of pores within the carbon block and its substantial size, the presence of trapped air within the carbon block structure, acting as an insulator or oxidant instead of the synthesizing liquid, poses a significant challenge to achieving uniform heat transfer. Therefore, it is crucial to guarantee homogeneous heat distribution throughout the entire structure during the aging process. Moreover, the conventional approach of sol-gel synthesis and impregnation within a Teflon-sealed autoclave leads to significant wastage of precursors and solvents, primarily due to the formation of THO outside the carbon block. That being stated, substituting the rigid stainless-steel Teflon-sealed autoclave with a flexible resistant pouch results in a better carbon block fitting inside the reaction chamber and fewer required chemicals for impregnation. Therefore, adopting an effective impregnation technique that addresses all the concerns mentioned above and enables sustainable and affordable impregnation processes becomes necessary.

The *Sous vide* technique involves integrating four essential sequential steps within a single “reactor” for efficient impregnation of the carbon block, including 1) applying a vacuum to remove air from the carbon block, 2) impregnating with precursors inside a flexible pouch rather than a rigid autoclave, 3) sealing the container to prevent oxygen intrusion, and 4) heating inside a water bath and eliminating any air from the process. Utilizing this method results in minimizing the requirement for large amounts of impregnation chemicals, preventing the contact between the synthesis solution and moisture in the air, and an efficient heat transfer throughout the carbon block structure using a hot water bath.<sup>21,22</sup> Consequently, the carbon block impregnated using the mentioned method attains uniform impregnation and formation of THO particles within its pores. Since the characteristics and advantages of the *Sous vide* technique align with the requirements for effectively impregnating the carbon block, we drew inspiration from this method to employ it for impregnating prefabricated carbon block filters. So, in this paper, the *Sous vide* term stands for an integrated four-in-one method to modify POU carbon block filters. We hypothesize that utilizing the integrated *Sous vide* method will reduce chemical consumption and promote an even distribution of THO particles within the carbon block.

The primary objective of this study is to impregnate a commercially available full-size carbon block filter with amorphous THO using the integrated steps provided by the *Sous vide* technique as a novel impregnation method. The novel and conventional autoclave impregnation approaches using our previously published sol-gel method were employed to synthesize amorphous THO directly within the carbon block. Subsequently, a series of characterization tests were conducted to assess the efficiency of the impregnation process using the novel method and to compare the crystallinity of the resulting THO with the conventional autoclave synthesis method. Lastly, the impregnated carbon blocks were utilized for POU arsenic removal from tap water spiked with arsenic and actual groundwater samples. Furthermore, the affordability of the technique was investigated.

## 2. Methodology

### 2.1. Chemicals and reagents

Titanium (IV) isopropoxide (TTIP) with a purity of 97%, pure ethyl alcohol (EtOH) with a grade of 190 proof (ACS Spectrophotometric grade, 95%), and sodium (meta)arsenite were obtained from Sigma Aldrich. Glacial acetic acid (Certified ACS Plus) was purchased from Fisher Chemicals. Sodium bicarbonate (ACS grade) was supplied by AMRESCO, and sodium arsenate (J. T. Baker, Dibasic, 7-Hydrate, ACS reagent) was acquired from J. T. Baker. All the chemicals and reagents were used as received without any further modifications.

### 2.2. Carbon block impregnation with THO

**2.2.1. Integrated *Sous vide* impregnation of the carbon block.**—The activated carbon block cartridges are manufactured by heating and extrusion of a mixture of powdered activated carbon and a polymer as the binder and wrapping the filter with one layer of plastic net.<sup>23</sup> Many types of cartridges are commercially available in the market, with different thicknesses, particle sizes, and types of activated carbon (e.g., lignite- vs bituminous coal-based). Figure S1 illustrates the prefabricated carbon block cartridge used in this study. A low titanium-containing activated carbon block (10" × 2.5", 5 μm) with the product number FI-ES-CAB10 was procured from APEC (CA, USA). To determine the porosity of the carbon block, a small cylindrical piece (obtained by drilling a volume of 17 cm<sup>3</sup>) was submerged in hot water, and the displaced water was measured using a graduated cylinder. The carbon block has a thickness of 1.3 cm, an outer diameter of 6.3 cm, an inner diameter of 3.6 cm, and a height of 24 cm. This results in a total volume of 480 cm<sup>3</sup> for the activated carbon block, with a void space of 244 cm<sup>3</sup> in the center. Based on the measured porosity of 68%, the carbon block possesses a total pore volume of 330 cm<sup>3</sup> (calculated as 480 × 0.68). Therefore, each carbon block module's net volume of the pores and void space is 574 cm<sup>3</sup> (or 1,148 cm<sup>3</sup> for two carbon blocks combined).

Figure 1 illustrates the dimensions of the carbon block and the process of impregnating it with amorphous THO using the *Sous vide* technique. The impregnation was conducted using commercial vacuum bags (FoodSaver 11" Heavy Duty rolls). The carbon blocks were not disassembled and were used as received, including the outer plastic mesh and rubber seal endcaps. Two carbon blocks were placed inside a single bag for simultaneous

impregnation. The sol-gel synthesis method was adapted from the literature with certain modifications.<sup>24,25</sup> Following the synthesis procedure described in our previous work, the ratios of the precursors and solvents were adjusted to achieve a total solution volume of 1,150 mL. Briefly, 340.7 mL of titanium isopropoxide (TTIP) and 387.8 mL of acetic acid were mixed and stirred for 75 minutes in a beaker. Subsequently, 421.5 mL of ethanol (EtOH) was added to the mixture. After stirring for 5 minutes, the solution was transferred to the vacuum bag containing the two carbon block modules. The vacuum bag containing the carbon blocks and the sol-gel synthesis solution was placed under the *Sous vide* vacuum and seal machine (NESCO Deluxe model VS-12). First, a vacuum was applied intermittently through pulses to evacuate the trapped air from the activated carbon block's pores and facilitate the solution penetration. This function was repeated until no further bubbling was observed. Next, the "Vacuum and Seal" function was utilized to apply a higher-intensity vacuum, followed by immediate bag sealing. To ensure proper sealing, an additional manual double seal was used. The sealed and vacuumed bag, containing the carbon blocks and the solution, was then placed in a preheated water bath at 80 °C. The aging step was performed for 20 hours inside the water bath. Afterward, the vacuum bag was cut open, and the carbon blocks were removed and dried overnight at 60 °C. Once dried, the carbon block was pre-washed with >18 Mohm nanopure (ThermoFisher, Barnstead GenPure) and inserted into a standard 12" × 4" housing for further washing with nanopure water at a continuous flow rate of 1 L/min for 30 minutes. The THO powders formed ex-situ to the carbon block were also collected, washed with EtOH and nanopure water, and dried at 60 °C overnight for further characterization tests.

**2.2.2. Conventional autoclave impregnation of the carbon block.**—The conventional autoclave synthesis was conducted using a small cylindrical piece of the carbon block (diameter of 3.1 cm and height of 2.3 cm) due to the larger size of the whole carbon block, which cannot fit inside a lab-scale autoclave. The objective was to compare the structure of the resulting THO between the two methods. The conventional autoclave method was performed in a manner similar to our previous work.<sup>16</sup> In brief, a cylindrical coupon of the carbon block with a volume of 17 cm<sup>3</sup> was obtained by cutting it using a drilling tool. Initially, 20.2 mL of TTIP was mixed with 23 mL of acetic acid and stirred for 75 minutes. Subsequently, 25 mL of EtOH was added to the solution. After stirring for 5 minutes, the carbon block piece was immersed in the solution, and a direct vacuum was applied to it using a vacuum pump. The solution and carbon block were then transferred to a Teflon-lined stainless-steel autoclave and aged in an oven at 80 °C for 20 hours. The impregnated carbon block was subsequently washed with ethanol and nanopure water and dried overnight at 60 °C. The same washing and drying procedures were carried out on the THO formed ex-situ to the carbon block, and the resulting powders were utilized for further characterization.

### 2.3. Pseudo-equilibrium batch experiments and continuous-flow arsenic removal tests

To determine the Freundlich isotherm parameters, batch experiments were conducted using the ex-situ collected THO powder within 50 mL centrifuge tubes. 15 μM arsenate (As(V)) or arsenite (As(III)) salts were spiked into Tempe tap water, which had a conductivity of 1,368 μS/cm and a pH of 7.9. Subsequently, adsorbent doses ranging from 12 to 144

mg/L were added to the tubes and shook them for a duration of 7 days. In the case of the arsenite experiments, the stock solution was purged with N<sub>2</sub> before adding arsenite to prevent any oxidation. After reaching equilibrium, we determined the arsenate and arsenite concentrations in the vials and fitted these data using the Freundlich isotherm equation ( $q_e = KC_e^{1/n}$ ),<sup>26</sup> where C<sub>e</sub> represents the equilibrium concentration of arsenate or arsenite in the solution (μg/L), q<sub>e</sub> is the adsorption capacity at equilibrium (μg/mg), K is the Freundlich adsorption capacity parameter ((μg/mg)(L/μg)<sup>1/n</sup>), and 1/n is the Freundlich adsorption intensity parameter (Unitless).

Figures S2 and S3 present the schematic design and a photograph of the setup utilized for the continuous POU treatment tests, respectively. The non-modified and THO-impregnated full-size carbon blocks were placed in separate POU continuous flow systems. A sediment filter was positioned before the carbon block module. Control tests confirmed that the sediment filter did not remove any arsenic. Water flowed through the carbon block module by gravity at a controlled flow rate of 1 L/min, regulated by a valve. The carbon block had an empty bed contact time (EBCT) of 28 seconds. The water passed through the system in daily cycles, consisting of 14 hours of continuous flow followed by 10 hours of stagnation with no flow, representing the intermittent water flow through a POU filter.

Two different water matrices containing arsenic were investigated in this study. One water matrix consisted of local tap water from Tempe, AZ (Table S2) with a conductivity of 1,368 μS/cm and a pH of 7.9, spiked with 100 μg/L of arsenate or arsenite. The same matrix was spiked with 10 μg/L of arsenate or arsenite to evaluate the effect of initial arsenic concentration, specifically to evaluate how the THO-carbon block system performs in reducing arsenic exposure even in drinking waters that comply with the existing arsenic MCL. For arsenite removal experiments, the feed barrels were purged with N<sub>2</sub> prior to adding arsenite to prevent any oxidation. The second water matrix was local groundwater, which served as a drinking water supply and had a conductivity of 1,132 μS/cm and a pH of 8.2 (Table S3). The groundwater contained 36 μg/L of arsenate and no arsenite. It is important to note that the municipality treats this groundwater to bring the arsenic concentration below the MCL of 10 μg/L. All experiments were conducted at a temperature of 23 ± 1 °C. Throughout the experiments, influent and effluent water samples were collected regularly.

#### 2.4. Analytical techniques and characterizing the impregnated carbon block

The crystallinity of the formed THO was examined using a powder X-ray diffractometer (XRD, PANalytical Aeries) to compare its structure with THO synthesized conventionally inside a Teflon-sealed autoclave. The titanium content of the impregnated carbon block was quantified through acid digestion of the samples, followed by analysis via an inductively coupled plasma mass spectrometer (ICP-MS, Perkin Elmer NexIon 1000). Briefly, the samples were digested using a mixture of H<sub>2</sub>SO<sub>4</sub> and HNO<sub>3</sub>, following the standard method 3030-G.<sup>27</sup> The titanium concentration was then measured using an ICP-MS. X-ray fluorescence (XRF) analysis (XL3, Thermo Scientific) was employed as a secondary method to confirm the titanium content. To investigate the homogeneity of the titanium coating inside the carbon block, elemental mapping was conducted using scanning electron



microscopy (SEM) coupled with energy-dispersive X-ray spectroscopy (EDX) on different parts of the carbon block (Helios 5, Thermo Fisher Scientific).

The metal concentration in the influent and effluent samples collected throughout the arsenic removal tests was quantified using ICP-MS. Before the analysis via ICP-MS, 4 mL of the samples were digested using 1 mL of a 10% HNO<sub>3</sub> solution, resulting in a final concentration of 2% HNO<sub>3</sub> in the digested samples.

### 3. Results and discussion

#### 3.1. Characterization of THO and Impregnated carbon block

XRD characterization provides evidence that the conditions of the vacuum-seal synthesis technique inside the pouch produce material that closely resembles those of the conventional autoclave synthesis approach. XRD analysis is usually applied for crystalline material characterization but is still often used as a preliminary technique to differentiate crystalline from amorphous structures. Thus, in our study, the XRD analysis provides preliminary confirmation for the presence of amorphous titanium (hydr)oxide materials.<sup>28,29</sup> Ongoing research is exploring other analytical tools, such as pair distribution function (PDF) and X-ray absorption fine structure (XAFS), as superior techniques to validate this finding and study the local structures.<sup>30-32</sup> The field of amorphous metal (hydr)oxide material science is still developing compared against well-established measurement and interpretation methods based upon crystalline materials.<sup>33</sup> Figure 2 presents the X-ray diffraction (XRD) spectra obtained from three samples: (1) THO powder that remained within the vacuum-seal bag but was formed outside the carbon block, (2) THO powder produced using a conventional Teflon-lined autoclave, and (3) commercial P25 as the reference crystalline TiO<sub>2</sub> to compare the crystalline peaks and facets. XRD analysis could not be performed on THO impregnated within the carbon block due to the formation of THO inside the pores of the porous carbon block and the relatively low titanium content compared to activated carbon. The XRD spectra of the two THO samples exhibit only a broad peak around 25°, which is indicative of amorphous titanium (hydr)oxide. Figure 2 includes a reference XRD pattern for crystalline TiO<sub>2</sub> to highlight the differences from the THO samples. The XRD spectra of the THO samples produced through the novel integrated method and conventional autoclave method are nearly identical.

Exposure of the synthesis solution to water or moisture increases the hydrolysis rate, forming a more crystalline structure.<sup>34</sup> No additional water was introduced during the synthesis process, so atmospheric moisture becomes the sole water source influencing the final product's structure. The employed novel impregnation technique effectively mitigates the contact between the synthesis solution and air or atmospheric water. The prompt sealing of the vacuum bag immediately after applying the vacuum plays a crucial role in preventing any moisture from coming into contact with the synthesis solution. This airtight sealing ensures the preservation of the desired moisture-free environment throughout the impregnation process.

Analysis of the THO-impregnated carbon block using acid digestion and consequent ICP-MS analysis revealed a titanium content of  $13 \pm 0.5$  wt.% as a result of the impregnation

process. This value agreed with the titanium loading obtained from XRF analysis as a secondary method. The titanium loading exhibited minimal variation, with a difference of less than 1% observed across nine distinct samples of the carbon block (i.e., 3 different spots at the top, middle, and bottom of the impregnated carbon block). The Ti loading in the wrapping plastic net was <1 wt.%.

Figure 3 presents SEM images and EDX elemental mapping of titania obtained from nine different regions of the carbon block. The mapping reveals that titanium particles are uniformly distributed throughout all sections of the filter. Matching the EDX elemental mapping with SEM images in Figure 3 depicts the presence of THO particles within the macropores and channels of the carbon block, which serve as pathways for water flow. The examples of THO particles inside the water pathways are pointed at by red arrows in Figure 3. Notable, not all surfaces of the activated carbon were covered by titanium materials, as these non-THO coated surfaces provide adsorption sites for the removal of organic contaminants, which we previously confirmed for the conventional sol-gel with a Teflon-lined bomb autoclave approach.<sup>16</sup> However, the size limitations of the Teflon vessel (diameter of 4.2 cm and height of 8 cm) restricted impregnation to small carbon block plugs, preventing full-scale impregnation of commercial carbon block samples. This size limitation was overcome by using the flexible vacuum pouches, which exhibited robustness and enabled the impregnation of carbon block samples of any size. Overall, the utilized impregnation process resulted in even titanium loading within the carbon block pores, with the uniform formation and distribution of THO particles achieved through the combined effects of vacuum and sealing and the homogenous heat transfer during the impregnation process.

### 3.2. Batch experiments and the obtained adsorption isotherms

Figure 4 shows the linearized form of the Freundlich isotherm ( $\log q_e = \log K + \frac{1}{n} \log C_e$ ),<sup>35</sup> derived from the measured equilibrium concentrations of arsenate and arsenite, and their corresponding adsorption capacities on the amorphous THO. In tap water, the Freundlich isotherm intensity parameter ( $1/n$ ) for arsenate and arsenite was found to be 0.37 and 0.5, respectively. These  $1/n$  values, below unity, suggest the heterogeneous nature of the adsorbent's surface after arsenate and arsenite adsorption, reflecting the different energies of the adsorption sites. Moreover,  $1/n < 1$  indicates the favorable adsorption of the sorbate,<sup>36</sup> in this case both arsenate and arsenite, over a wide range of concentrations in tap water by the synthesized amorphous THO.<sup>37</sup> In essence, the obtained  $1/n$  values less than unity demonstrate the capability of the synthesized adsorbent to effectively remove arsenate and arsenite, even at very low concentrations,<sup>38</sup> which is a significant advantage in reducing exposure to arsenic at lower levels. In addition, arsenite is often more difficult to remove due to its neutral charge at environmentally-relevant pH values.<sup>39</sup> Additionally, the removal of arsenite by the THO-carbon block during batch tests was surprisingly efficient, especially considering that most work on iron-based adsorbents typically favors arsenate over arsenite adsorption. This finding underscores an advantage of the synthesized THO when compared to conventionally used iron-based media, which often exhibit low arsenic adsorption capacities at low initial concentrations.<sup>9,10</sup> This intriguing discovery in batch experiments



was subsequently corroborated in continuous flow column experiments, as elaborated upon in conjunction with Figure 5.

Oxo-anions, including arsenic, adsorb onto metal (hydr)oxides through surface inner-sphere complexation and oxygen bridging.<sup>40</sup> Likewise, other co-occurring oxo-anions can compete with arsenic for adsorption.<sup>12</sup> Among these, phosphate stands out as a significant competitor for arsenate due to its similar acidity, charge, and geometry. Even though the phosphate concentrations in the studied tap water were too low to effectively compete with arsenic (6 µg P/L), we conducted batch experiments using equimolar concentrations of phosphate and arsenate (15 µM) to examine the selectivity of the THO adsorbent. The results revealed that the synthesized THO had an arsenate adsorption capacity of 6.8 µg/mg (0.09 µmoleAs/mg), and a phosphate adsorption capacity of 2.3 µg/mg (0.07 µmoleP/mg). These findings demonstrate that the synthesized THO adsorbent exhibits a slightly higher affinity for adsorbing arsenate compared to phosphate. To quantitatively assess this selectivity, the equimolar based binary separation factor ( $\alpha_{\text{target ion} / \text{competing ion}} = \frac{q_t C_{e,c}}{q_c C_{e,t}}$ ) was calculated to be 30, which illustrates the higher selectivity of the amorphous THO towards arsenate (i.e.,  $\alpha > 1$ ).<sup>41</sup> This selectivity is a notable advantage of the developed filter, as it can selectively adsorb hazardous arsenic even in the presence of its competitive counterpart.

### 3.3. POU arsenic removal tests with THO-impregnated carbon block

Figure 5a illustrates the arsenate breakthrough curve obtained from treating 100 µg/L arsenic-spiked tap water using the THO-impregnated carbon block over the treatment of 10,000 bed volumes (BV). In our study, one bed volume corresponds to 0.48 liters of water for the full-sized carbon block utilized. The THO carbon block demonstrated exceptional arsenate and arsenite removal efficiency, surpassing 90%, during the initial 2,000 and 4,000 BV of treatment, respectively. This level of efficiency resulted in reducing influent concentrations to levels below the MCL of 10 µg/L. However, a decrease in arsenic adsorption was observed in the subsequent BVs of treated water, leading to a breakthrough. After treating 10,000 BV of water, it was determined that the cumulative amount of arsenate and arsenite removed from the water, representing a reduction in exposure if the water were to be used for drinking, was 224 mg and 260 mg of arsenic, respectively. This calculation was based on the area above the breakthrough curve, taking into account the volume of each BV. Consequently, after the treatment of 10,000 BV, the adsorption capacity of the THO-impregnated carbon block was found to be 4.6 mg As/g Ti or 0.6 mg As/g THO-carbon block for arsenate, and 5.3 mg As/g Ti or 0.7 mg As/g THO-carbon block for arsenite. This observation highlights a higher arsenite adsorption capacity and a delayed breakthrough compared to arsenate, demonstrating the greater selectivity of the developed filter toward arsenite, particularly at the initial concentration of 100 µg/L. Phosphate is a well-known competitor for arsenate, and its presence in drinking water could result in a faster arsenate breakthrough.<sup>42</sup> Since phosphate concentration in the tap water was only 6 µg/L as P, which is too low to compete with arsenate, other competing ions, such as silicate, likely cause a lower selectivity towards arsenate and is a focus on ongoing research on the THO surface.

The arsenate breakthrough point is almost similar to the observations in our previous work, where a small cylindrical piece of carbon block was impregnated through a conventional method of using a Teflon-sealed autoclave as the reactor.<sup>16</sup> In addition, the arsenate adsorption capacity of the full-size impregnated carbon block after the treatment of 10,000 BV in this study (4.6 mg As/g Ti) is comparable with that of bench-scale 17 cm<sup>3</sup> carbon block plug (4.1 mg As/g Ti) obtained in our previous study.<sup>16</sup>

The semi-steep nature of the breakthrough curve suggests that while impregnation occurred throughout the macropores, mesopores, and micropores of the carbon block, it primarily took place within the macropores and water pathway channels. This localization of impregnation within these pathways results in an enhanced mass transfer coefficient.<sup>43</sup> This is in line with a general principle concerning porous adsorbents like carbon blocks, where pore size plays a significant role in shaping the mass transfer zone in continuous flow. Micropores, due to their small size, offer access to a substantial portion of the intraparticle surface area, but their size leads to low mass transfer diffusion rates, primarily due to surface interactions and tortuosity.<sup>44</sup> Consequently, it becomes more challenging for the sorbate to reach the adsorption sites within the micropores, resulting in intraparticle diffusion-limited adsorption and a gradual breakthrough. In contrast, sorbate molecules can more easily reach the adsorption sites in the macropores and water pathway channels, leading to bulk or film transfer diffusion limitation and a steeper breakthrough.<sup>45</sup> Given the semi-steep breakthrough shape of the curve, it can be inferred that the adsorption predominantly occurred within the macropores and water pathway channels of the carbon block. The findings agree with the combined Biot number of 32 reported in our previous work.<sup>16</sup> Given that a Biot number between 1 and 100 suggests a combination of intraparticle diffusion and film mass transfer-controlled adsorption,<sup>46</sup> lower values in this range show more importance of film mass transfer limitation. Furthermore, the similarity in adsorption capacities and breakthrough shapes between the full-sized impregnated carbon block and lab-scale coupons, as reported in our previous work, indicates the effectiveness of the integrated method used to scale up production of the THO-impregnated carbon block.<sup>16</sup> Additionally, because the developed system is designed as a POU technology that can accommodate different flow rates, the mass transfer zone is influenced by varying flow rates. Lower flow rates result in a reduced mass transfer zone velocity and longer EBCT, leading to a delayed and more gradual breakthrough. In this study, to align with typical POU operations, a flow rate of 1 L/min was selected, providing an EBCT of 28 seconds, which falls within the common range for POU systems (<1 minute).<sup>47</sup>

A minimal hydraulic pressure drop (< 0.35 bar or < 5 psi) was observed during the operation of either the non-treated or impregnated carbon block. This indicates that the impregnation process with THO did not cause any pore blockage in the carbon block, allowing water to flow through the pores without obstruction. Furthermore, continuous titanium (Ti) concentration monitoring during water flow showed no evidence of Ti leaching (i.e., < 1 ppb). The homogeneous heating achieved during the aging step played a crucial role in the formation of THO particles inside the carbon block and their strong binding with the carbon surface, thereby preventing the leaching of Ti from the impregnated carbon block. Another reason for the essential Ti stability on the carbon surface is the disposal of the filter after exhaustion. Adsorption treatment processes transfer pollutants from liquid to a solid

phase, which can be easily disposed of in landfills, thereby removing them from common exposure pathways to the environment and people. For home POU systems, regeneration of THO-carbon block probably isn't a viable route. Iron- and some other metal oxide adsorption systems used in POE arsenic treatment processes can be regenerated using heated strong alkaline solutions.<sup>48,49</sup> Because these solutions generate hazardous waste containing arsenic, they are not recommended for home POU systems. There is a potential advantage in using titanium instead of iron-impregnated carbon blocks that could be explored in the future through end-of-life landfill leaching tests. As we have discussed and demonstrated in our previous work, arsenic binds to the THO surface through oxygen binding, which involves a chemical inner-sphere complexation.<sup>16</sup> This chemical interaction between arsenic and THO results in irreversible and stable adsorption of arsenic. Moreover, in comparison to iron-modified carbon, the strong chemical bonding established between the THO particles and the carbon surface, achieved through the sol-gel synthesis method, prevents any leaching of titanium or arsenic. This ensures that the filter remains safe for disposal in landfills, as originally designed for carbon block filters.

Figure 5a also presents the arsenic breakthrough curves for the THO-impregnated carbon block obtained from treating arsenic-spiked tap water that contains only 10 µg/L. Impressively, the THO-impregnated carbon block achieved the removal of over 90% of both arsenate and arsenite over the first 5,000 and 10,000 BV, respectively, resulting in an effluent concentration below 1 µg/L. Over the 10,000 BV treatment of the 10 µg/L arsenic-spiked tap water, the THO-impregnated carbon block effectively removed arsenate and arsenite, equivalent to 38 and 43 mg of arsenic, respectively. These values correspond to an adsorption capacity of 0.8 mg As/g Ti or 0.1 mg As/g THO-carbon block for arsenate and 0.9 mg As/g Ti or 0.1 mg As/g THO-carbon block for arsenite. The extended excellent performance of the system with an influent arsenic concentration of 10 µg/L demonstrates the feasibility of reducing long-term exposure and health risks, even at lower concentrations of arsenic, which fall at or below the current arsenic MCL. The substantial amounts of removed arsenic highlight the necessity of employing POU treatment systems as a secondary barrier for arsenic removal from drinking water.

Drawing from the literature, Fe-based adsorbents typically exhibit arsenic adsorption capacities ranging from 0.2 to 280 mmole As/mole Fe (Table S1). Taken with caution, the higher end of this capacity range is achieved through unrealistically high initial concentrations, sometimes reaching up to 140,000 µg/L. Therefore, a valuable comparison can be made by examining these adsorbents on a molar basis when evaluating their performance at similar influent concentrations. In the case of the THO-impregnated carbon block developed in this study, the arsenate and arsenite adsorption capacities stand at 3 and 3.4 mmole As/mole Ti, respectively, when considering waters with an influent concentration on only 100 µg/L. In contrast, certain Fe-based adsorbents have demonstrated capacities in the range of 1.1 to 2 mmole As/mole Fe at similar influent concentrations.<sup>50,51</sup> These molar-based capacities underscore the superior performance of the developed THO-impregnated carbon block in comparison to several Fe-based adsorbents, particularly when dealing with realistic concentrations. To the best of our knowledge, there are no studies conducted at the initial concentration of 10 µg/L for comparison, mainly because most researchers consider the MCL of 10 µg/L as the remediation goal. Additionally, the

adsorption capacities in this study were determined using tap water, which contains various competing ions, while many of the reported adsorption capacities in the literature are derived from experiments conducted with synthetic water matrices. The superior efficiency of the developed THO-impregnated carbon block in removing arsenate and arsenite from such very low concentrations (i.e., 10 µg/L) positions it as a potential alternative to the existing Fe-based adsorbents, which are typically employed at higher concentrations.

Figure 5b illustrates the arsenic breakthrough curve obtained from treating groundwater containing 36 µg/L of ambient arsenic (100% arsenate) using the THO-impregnated carbon block. Over the course of treating the first ~3,000 BV, more than 90% of the influent arsenic was successfully removed, demonstrating effective arsenic removal. Subsequently, a gradual breakthrough of arsenic occurred. After treating 6,000 BV of water, the THO carbon block achieved a total arsenic removal of 81 mg (corresponding to 1.7 mg As/g Ti or 0.2 mg As/g THO-carbon block). These values are comparable to the adsorption capacity observed in the arsenate-spiked tap water experiments with a 3 times higher influent arsenate concentration (4.6 mg As/g Ti or 0.6 mg As/g THO-carbon block) and 10,000 BV treatment. This indicates that the impregnated carbon block exhibits effective arsenic removal capabilities across different influent arsenic concentrations.

Because other hazardous oxo-anions and metals co-occur in groundwater naturally,<sup>52</sup> there could be an antagonistic health effect due to long-term exposure to their mixtures.<sup>53,54</sup> In addition to arsenic, the public groundwater supply contained detectable levels of selenium, vanadium, and iron. Figure S4 reveals that the unmodified carbon block did not exhibit significant removal of As, Se, V, or Fe within the initial 250 BV of the treatment, prompting the discontinuation of further testing with the unmodified carbon block. In contrast, Figure 5b demonstrates the simultaneous removal of these metals, including arsenic, by the THO-impregnated carbon block. While selenium removal was not as efficient as arsenic removal, the THO carbon block achieved substantial removal of vanadium and iron. The removal of iron is advantageous for two reasons. Iron can contribute to aesthetic issues such as tap water color and staining. Additionally, the removal of iron by the THO carbon block may potentially enhance arsenic removal through the coprecipitation of arsenic with pre-existing iron present within the pores of the carbon block.<sup>55</sup> In fact, the irregular shape of the breakthrough curve for arsenic may be attributed, in part, to the adsorption of arsenate onto the removed iron. Simultaneous removal of vanadium is the other advantage of the impregnated carbon block. While vanadium does not currently have the United States Environmental Protection Agency (USEPA) MCL, recent research indicates that vanadium is an emerging drinking water contaminant that raises health concerns.<sup>56</sup> Overall, the integrated features involved in *Sous vide* impregnation resulted in the proper formation of amorphous THO inside the carbon block's pores, comparable to the THO formed through the conventional Teflon-sealed autoclave approach.

### 3.4. Chemical Precursor Consumption in integrated *Sous vide* vs Conventional Synthesis Approaches

The impregnation technique used in this study addresses a critical need in terms of reducing chemical waste, resulting in a more affordable and environmentally friendly process. Table

1 provides a comparison of the total volume of chemicals required for impregnating a carbon block using the conventional autoclave method versus the *Sous vide* technique. Concerning the volume of the small 17 cm<sup>3</sup> carbon block piece and a full-size carbon block filter (480 cm<sup>3</sup>), impregnation of the full-size carbon block via the conventional autoclave method requires 3,887 mL of synthesis solution (details are explained in the SI). In contrast, impregnation within a flexible pouch consumed only 1,150 mL of synthesis solution, which is 70% lower than the volume required for conventional impregnation. This significant reduction in chemical consumption translates to higher affordability and a more sustainable process. Overall, the current integrated impregnation technique successfully produces a THO-impregnated carbon block with comparable arsenic removal performance to conventional impregnation, utilizing a 70% lower volume of precursor chemicals. This reduces the costs of the initial chemicals but also the costs and impacts of disposing of residual chemicals after the synthesis of the THO-impregnated carbon block is completed.

### 3.5. Environmental Implications

Amorphous THO-impregnated carbon block modules have been demonstrated as reliable point-of-use (POU) filters for the effective removal of arsenic from drinking water, with no adverse effects on the hydraulic flow rate or leaching of precursor materials. THO-impregnated carbon block continued the ability to remove trace organics.<sup>16</sup> The application of the integrated impregnation technique that involves applying a vacuum, impregnation inside a flexible pouch, sealing the container, and heating inside a water bath successfully eliminates trapped oxygen, allowing the synthesis solution to penetrate the carbon block pores. The absence of air and the homogenous reaction environment provided by the hot water bath contribute to the even distribution of THO particles with ~13 wt.% Ti within the carbon block pores without obstructing water pathways or causing a significant hydraulic pressure drop.

The modified carbon block exhibits promising performance in removing arsenate, arsenite, and other hazardous oxo-anions and metals from both spiked tap water and actual groundwater, comparable to conventional bench-scale autoclave methods. The capability of the developed THO-impregnated carbon block in the efficient removal of both arsenate and arsenite from very low concentrations of the feed water makes the technology outstanding compared to the existing iron-based adsorbent media. This is particularly of high importance since several governments are seeking lower MCL for arsenic in drinking water.<sup>57</sup> Therefore, the development of such filters that can adsorb both arsenate and arsenite in super-low concentrations is an emerging necessity. The appropriate sol-gel reaction progression inside the vacuum bag results in a chemical binding between THO and the carbon surface, preventing Ti from leaching during water flow. Additionally, the integrated impregnation process reduces chemical consumption by 70%, offering a more sustainable and affordable approach for modifying carbon block filters with amorphous THO.

Currently, there are commercially available POE and POU arsenic removal systems (e.g., AdEdge Bayoxide<sup>®</sup> E33 Arsenic Filter and AD4510S AdEdge Arsenic Removal Water Filter), with many of them utilizing iron-based granular adsorbent media. These iron-based POU systems typically serve a single function, specifically the removal of arsenic, and do

not address the removal of organic pollutants or taste/odor compounds. Impregnating metal (hydr)oxides into an activated carbon block enables the development of a multi-functional POU system. This is a significant advantage in reducing the overall space requirements beneath the sink. In unpublished work by our lab, an evaluation of a commercially available iron-impregnated carbon block obtained from Asia indicated the prolonged release of soluble iron, at levels above the secondary maximum contaminant level of 0.3 mg/L, into the treated water. Iron release had adverse aesthetic effects of POU systems. In contrast, impregnating the carbon block with THO did not result in any titanium leaching and Ti level in the effluent was always below 1 µg/L.

Other POU designs capable of removing arsenic that use nanofiltration or reverse osmosis often exhibit low water recovery (~30%)<sup>14</sup> and discharge arsenic to the sewer or septic system. These membrane-based POU systems also require cartridge filters and carbon block pretreatment to remove particulates and disinfectant residuals. Additionally, they demand significantly more space than a single THO-carbon block cartridge. In contrast to membrane-based POU systems, carbon block POU designs that have zero liquid waste and dispose of solid waste containing arsenic (i.e., spent carbon block) to landfills. Consequently, the THO-carbon block presented in this study offers a substantial improvement over other POU systems for arsenic removal. Future research is required to study the potential application of the same technique for retrofitting other types of porous media with different dopants or target contaminants, which could expand the range of water treatment options available.

## Supplementary Material

Refer to Web version on PubMed Central for supplementary material.

## Acknowledgments

National Science Foundation Engineering Education and Centers (EEC-1449500) partially funded this work. The authors acknowledge using facilities within the Eyring Materials Center at Arizona State University, supported partly by the National Science Foundation (NNCI-ECCS-2025490). In addition, the research reported was partially supported by the National Institute of Environmental Health Sciences through the Metals and metal mixtures: cognitive aging, remediation, and exposure sources (MEMCARE) center [P42ES030990]. The content is solely the authors' responsibility and does not necessarily represent the official views of the National Institutes of Health.

## References

- (1). Abejón R; Garea A A Bibliometric Analysis of Research on Arsenic in Drinking Water during the 1992-2012 Period: An Outlook to Treatment Alternatives for Arsenic Removal. *Journal of Water Process Engineering* 2015, 6, 105–119. 10.1016/j.jwpe.2015.03.009.
- (2). Foster SA; Pennino MJ; Compton JE; Leibowitz SG; Kile ML Arsenic Drinking Water Violations Decreased across the United States Following Revision of the Maximum Contaminant Level. *Environ Sci Technol* 2019, 53 (19), 11478–11485. 10.1021/acs.est.9b02358. [PubMed: 31502444]
- (3). Gifford M; Chester M; Hristovski K; Westerhoff P Human Health Tradeoffs in Wellhead Drinking Water Treatment: Comparing Exposure Reduction to Embedded Life Cycle Risks. *Water Res* 2018, 128, 246–254. 10.1016/j.watres.2017.10.014. [PubMed: 29107909]
- (4). Soler-Blasco R; Llop S; Riutort-Mayol G; Lozano M; Vallejo-Ortega J; Murcia M; Ballester F; Irizar A; Andiarrena A; Fernandez-Jimenez N; Braeuer S; Harari F Genetic Susceptibility to Neurotoxicity Related to Prenatal Inorganic Arsenic Exposure in Young Spanish Children.



Environ Sci Technol 2023, 57 (41), 15366–15378. 10.1021/acs.est.3c03336. [PubMed: 37787746]

- (5). Martinez-Morata I; Bostick BC; Conroy-Ben O; Duncan DT; Jones MR; Spaur M; Patterson KP; Prins SJ; Navas-Acien A; Nigra AE Nationwide Geospatial Analysis of County Racial and Ethnic Composition and Public Drinking Water Arsenic and Uranium. Nat Commun 2022, 13 (1). 10.1038/s41467-022-35185-6.
- (6). Westerhoff P; De Haan M; Martindale A; Badruzzaman M Arsenic Adsorptive Media Technology Selection Strategies; 2006. 41. <http://iwaponline.com/wqrj/article-pdf/41/2/171/230081/wqrjc0410171.pdf>.
- (7). Spayd SE; Robson MG; Buckley BT Whole-House Arsenic Water Treatment Provided More Effective Arsenic Exposure Reduction than Point-of-Use Water Treatment at New Jersey Homes with Arsenic in Well Water. Science of the Total Environment 2015, 505, 1361–1369. 10.1016/j.scitotenv.2014.06.026. [PubMed: 24975493]
- (8). Hering JG; Katsoyiannis IA; Theoduloz GA; Berg M; Hug SJ Arsenic Removal from Drinking Water: Experiences with Technologies and Constraints in Practice. Journal of Environmental Engineering 2017, 143 (5). 10.1061/(asce)ee.1943-7870.0001225.
- (9). Bai Y; Tang X; Sun L; Yin W; Hu G; Liu M; Gong Y Application of Iron-Based Materials for Removal of Antimony and Arsenic from Water: Sorption Properties and Mechanism Insights. Chemical Engineering Journal 2022, 431 (P2), 134143. 10.1016/j.cej.2021.134143.
- (10). Hao L; Liu M; Wang N; Li G A Critical Review on Arsenic Removal from Water Using Iron-Based Adsorbents. RSC Adv 2018, 8 (69), 39545–39560. 10.1039/c8ra08512a. [PubMed: 35558047]
- (11). Abraham Chen, by S.; Lal V; Wang L Arsenic Removal from Drinking Water by Point of Entry/Point of Use Adsorptive Media U.S. EPA Demonstration Project at Oregon Institute of Technology at Klamath Falls, OR Final Performance Evaluation Report; 2011.
- (12). Pincus LN; Rudel HE; Petrovi PV; Gupta S; Westerhoff P; Muhich CL; Zimmerman JB Exploring the Mechanisms of Selectivity for Environmentally Significant Oxo-Anion Removal during Water Treatment: A Review of Common Competing Oxo-Anions and Tools for Quantifying Selective Adsorption. Environ Sci Technol 2020, 9769–9790. 10.1021/acs.est.0c01666. [PubMed: 32515947]
- (13). Herkert NJ; Merrill J; Peters C; Bollinger D; Zhang S; Hoffman K; Ferguson PL; Knappe DRU; Stapleton HM Assessing the Effectiveness of Point-of-Use Residential Drinking Water Filters for Perfluoroalkyl Substances (Pfass). Environ Sci Technol Lett 2020, 7 (3), 178–184. 10.1021/acs.estlett.0c00004.
- (14). Chen B; Jiang J; Yang X; Zhang X; Westerhoff P Roles and Knowledge Gaps of Point-of-Use Technologies for Mitigating Health Risks from Disinfection Byproducts in Tap Water: A Critical Review. Water Research 2021. 10.1016/j.watres.2021.117265.
- (15). Wu C-C; Love NG; Olson TM Bacterial Transmission and Colonization in Activated Carbon Block (ACB) Point-of-Use (PoU) Filters. Environ Sci (Camb) 2021, 7 (6), 1114–1124. 10.1039/d0ew00982b.
- (16). Farsad A; Niimi K; Ersan MS; Gonzalez-Rodriguez JR; Hristovski KD; Westerhoff P Mechanistic Study of Arsenate Adsorption onto Different Amorphous Grades of Titanium (Hydr)Oxides Impregnated into a Point-of-Use Activated Carbon Block. ACS ES and T Engineering 2023, 3 (7), 989–1000. 10.1021/acsestengg.3c00012. [PubMed: 37546364]
- (17). Laurindo JB; Stringari GB; Paes SS; Carciofi BAM Experimental Determination of the Dynamics of Vacuum Impregnation of Apples. J Food Sci 2007, 72 (8). 10.1111/j.1750-3841.2007.00512.x.
- (18). Badillo GM; Segura LA; Laurindo JB Theoretical and Experimental Aspects of Vacuum Impregnation of Porous Media Using Transparent Etched Networks. International Journal of Multiphase Flow 2011, 37 (9), 1219–1226. 10.1016/j.ijmultiphaseflow.2011.06.002.
- (19). Hanaor DAH; Chironi I; Karatchevtseva I; Triani G; Sorrell CC Single and Mixed Phase TiO<sub>2</sub> Powders Prepared by Excess Hydrolysis of Titanium Alkoxide. Advances in Applied Ceramics 2012, 111 (3), 149–158. 10.1179/1743676111Y.0000000059.

- (20). Wetchakun N; Phanichphant S Effect of Temperature on the Degree of Anatase-Rutile Transformation in Titanium Dioxide Nanoparticles Synthesized by the Modified Sol-Gel Method. *Current Applied Physics* 2008, 8 (3–4), 343–346. 10.1016/j.cap.2007.10.028.
- (21). Baldwin DE Sous Vide Cooking: A Review. *Int J Gastron Food Sci* 2012, 1 (1), 15–30. 10.1016/j.ijgfs.2011.11.002.
- (22). Przybylski W; Jaworska D; Kajak-Siemaszko K; Sałek P; Pakuła K Effect of Heat Treatment by the Sous-Vide Method on the Quality of Poultry Meat. *Foods* 2021, 10 (7). 10.3390/foods10071610.
- (23). Braslavskaya Y; Ponomarev V; Mitchenko T; Maletskyi Z; Kosogina I Production Technology and Filtering Properties of Carbon Block Cartridges. *Water and Water Purification Technologies. Scientific and Technical News* 2022, 33 (2), 32–42. 10.20535/2218-930022022255835.
- (24). Bahtat A; Bouazaoui M; Bahtat M; Garapon C; Jacquier B; Mugnier J Up-Conversion Fluorescence Spectroscopy in  $\text{Er}^{3+}$ :  $\text{TiO}_2$  Planar Waveguides Prepared by a Sol-Gel Process. *J Non Cryst Solids* 1996, 202 (1–2), 16–22. 10.1016/0022-3093(96)00172-X.
- (25). Doeuff S; Henry M; Sanchez C; Livage J Hydrolysis of Titanium Alkoxides: Modification of the Molecular Precursor by Acetic Acid. *J Non Cryst Solids* 1987, 89 (1–2), 206–216. 10.1016/S0022-3093(87)80333-2.
- (26). Freundlich H. Über Die Adsorption in Lösungen. *Zeitschrift für Physikalische Chemie* 1907, 57U (1), 385–470. 10.1515/zpch-1907-5723.
- (27). Westerhoff P; Song G; Hristovski K; Kiser MA Occurrence and Removal of Titanium at Full Scale Wastewater Treatment Plants: Implications for  $\text{TiO}_2$  Nanomaterials. *Journal of Environmental Monitoring* 2011, 13 (5), 1195–1203. 10.1039/c1em10017c. [PubMed: 21494702]
- (28). Deng S; Li Z; Huang J; Yu G Preparation, Characterization and Application of a Ce-Ti Oxide Adsorbent for Enhanced Removal of Arsenate from Water. *J Hazard Mater* 2010, 179 (1–3), 1014–1021. 10.1016/j.jhazmat.2010.03.106. [PubMed: 20403658]
- (29). Zhang W; Liu C; Wang L; Zheng T; Ren G; Li J; Ma J; Zhang G; Song H; Zhang Z; Li Z A Novel Nanostructured Fe-Ti-Mn Composite Oxide for Highly Efficient Arsenic Removal: Preparation and Performance Evaluation. *Colloids Surf A Physicochem Eng Asp* 2019, 561, 364–372. 10.1016/j.colsurfa.2018.10.077.
- (30). Lan S; Zhu L; Wu Z; Gu L; Zhang Q; Kong H; Liu J; Song R; Liu S; Sha G; Wang Y; Liu Q; Liu W; Wang P; Liu CT; Ren Y; Wang XL A Medium-Range Structure Motif Linking Amorphous and Crystalline States. *Nat Mater* 2021, 20 (10), 1347–1352. 10.1038/s41563-021-01011-5. [PubMed: 34017117]
- (31). Terban MW; Billinge SJL Structural Analysis of Molecular Materials Using the Pair Distribution Function. *Chemical Reviews* 2022, 1208–1272. 10.1021/acs.chemrev.1c00237. [PubMed: 34788012]
- (32). Yang Y; Zhou J; Zhu F; Yuan Y; Chang DJ; Kim DS; Pham M; Rana A; Tian X; Yao Y; Osher SJ; Schmid AK; Hu L; Ercius P; Miao J Determining the Three-Dimensional Atomic Structure of an Amorphous Solid. *Nature* 2021, 592 (7852), 60–64. 10.1038/s41586-021-03354-0. [PubMed: 33790443]
- (33). Li L; Shao Q; Huang X Amorphous Oxide Nanostructures for Advanced Electrocatalysis. *Chemistry - A European Journal*. 2020, 3943–3960. 10.1002/chem.201903206. [PubMed: 31483074]
- (34). McDonagh C; Sheridan F; Butler T; Macraith BD Characterisation of Sol-Gel-Derived Silica Films. 1996, 194.
- (35). Modaresahmadi K; Khodadoust AP; Wescott J Adsorption of Fluoride from Water Using Aluminum Coated Sand: Kinetics, Equilibrium, Effect of PH, and Coexisting Ions. *Journal of Geoscience and Environment Protection* 2022, 10 (12), 224–241. 10.4236/gep.2022.1012013.
- (36). Modaresahmadi K; Khodadoust A; Wescott J Adsorption of Fluoride from Water Using Al–Mg–Ca Ternary Metal Oxide-Coated Sand. *Water Supply* 2023. 10.2166/ws.2023.269.
- (37). Markovski J; Hristovski KD An Experimental Approach for Determining Thermodynamic Surface Complexation Descriptors of Weak-Acid Oxyanions onto Metal (Hydr)Oxides: Case Study of Arsenic and Titanium Dioxide. *Science of the Total Environment* 2019, 677, 167–174. 10.1016/j.scitotenv.2019.04.352. [PubMed: 31055097]

- (38). Hristovski KD; Markovski J Engineering Metal (Hydr)Oxide Sorbents for Removal of Arsenate and Similar Weak-Acid Oxyanion Contaminants: A Critical Review with Emphasis on Factors Governing Sorption Processes. *Science of the Total Environment* 2017, 598, 258–271. 10.1016/j.scitotenv.2017.04.108. [PubMed: 28445823]
- (39). Pena M; Meng X; Korfiatis GP; Jing C Adsorption Mechanism of Arsenic on Nanocrystalline Titanium Dioxide. *Environ Sci Technol* 2006, 40 (4), 1257–1262. 10.1021/es052040e. [PubMed: 16572784]
- (40). Yamani JS; Miller SM; Spaulding ML; Zimmerman JB Enhanced Arsenic Removal Using Mixed Metal Oxide Impregnated Chitosan Beads. *Water Res* 2012, 46 (14), 4427–4434. 10.1016/j.watres.2012.06.004. [PubMed: 22743162]
- (41). Yamani JS; Lounsbury AW; Zimmerman JB Towards a Selective Adsorbent for Arsenate and Selenite in the Presence of Phosphate: Assessment of Adsorption Efficiency, Mechanism, and Binary Separation Factors of the Chitosan-Copper Complex. *Water Res* 2016, 88, 889–896. 10.1016/j.watres.2015.11.017. [PubMed: 26613182]
- (42). Wielinski J; Jimenez-Martinez J; Göttlicher J; Steininger R; Mangold S; Hug SJ; Berg M; Voegelin A Spatiotemporal Mineral Phase Evolution and Arsenic Retention in Microfluidic Models of Zerovalent Iron-Based Water Treatment. *Environ Sci Technol* 2022, 56 (19), 13696–13708. 10.1021/acs.est.2c02189. [PubMed: 36095156]
- (43). Poursaeidesfahani A; Andres-Garcia E; de Lange M; Torres-Knoop A; Rigutto M; Nair N; Kapteijn F; Gascon J; Dubbeldam D; Vlucht TJH Prediction of Adsorption Isotherms from Breakthrough Curves. *Microporous and Mesoporous Materials* 2019, 277, 237–244. 10.1016/j.micromeso.2018.10.037.
- (44). Luo J; Fu K; Yu D; Hristovski KD; Westerhoff P; Crittenden JC Review of Advances in Engineering Nanomaterial Adsorbents for Metal Removal and Recovery from Water: Synthesis and Microstructure Impacts. *ACS ES&T Engineering* 2021, 1 (4), 623–661. 10.1021/acsestengg.0c00174.
- (45). Hand DW; Crittenden JC; Asce M; Thacker WE Simplified Models for Design of Fixed-Bed Adsorption Systems. *Journal of Environmental Engineering* 1984, 110 (2), 440–456.
- (46). Traegner UK; Suidan MT Parameter Evaluation for Carbon Adsorption. *Journal of Environmental Engineering* 1989, 115 (1), 109–128. 10.1061/(ASCE)0733-9372(1989)115:1(109).
- (47). Wang Z; Bi X; He X; Xie Y; Lin J; Deng B A Two-Sorbent System for Fast Uptake of Arsenate from Water: Batch and Column Studies. *Water Res* 2023, 228. 10.1016/j.watres.2022.119290.
- (48). Sorg TJ; Chen ASC; Wang L; Kolisz R Regenerating an Arsenic Removal Iron-Based Adsorptive Media System, Part 1: The Regeneration Process. *Journal - American Water Works Association*. 2017, 13–24. 10.5942/jawwa.2017.109.0045.
- (49). Sylvester P; Westerhoff P; Möller T; Badruzzaman M; Boyd O A Hybrid Sorbent Utilizing Nanoparticles of Hydrous Iron Oxide for Arsenic Removal from Drinking Water. *Environ Eng Sci* 2007, 24 (1), 104–112. 10.1089/ees.2007.24.104.
- (50). Kalaruban M; Loganathan P; Nguyen TV; Nur T; Hasan Jahir MA; Nguyen TH; Trinh MV; Vigneswaran S Iron-Impregnated Granular Activated Carbon for Arsenic Removal: Application to Practical Column Filters. *J Environ Manage* 2019, 239, 235–243. 10.1016/j.jenvman.2019.03.053. [PubMed: 30903835]
- (51). Banerjee K; Amy GL; Prevost M; Nour S; Jekel M; Gallagher PM; Blumenschein CD Kinetic and Thermodynamic Aspects of Adsorption of Arsenic onto Granular Ferric Hydroxide (GFH). *Water Res* 2008, 42 (13), 3371–3378. 10.1016/j.watres.2008.04.019. [PubMed: 18538818]
- (52). Coyte RM; Vengosh A Factors Controlling the Risks of Co-Occurrence of the Redox-Sensitive Elements of Arsenic, Chromium, Vanadium, and Uranium in Groundwater from the Eastern United States. *Environ Sci Technol* 2020, 54 (7), 4367–4375. 10.1021/acs.est.9b06471. [PubMed: 32167307]
- (53). Stoiber T; Temkin A; Andrews D; Campbell C; Naidenko OV Applying a Cumulative Risk Framework to Drinking Water Assessment: A Commentary. *Environmental Health: A Global Access Science Source*. 2019. 10.1186/s12940-019-0475-5.

- (54). Thompson AK; Monti MM; Gribble MO Co-Occurrence of Metal Contaminants in United States Public Water Systems in 2013–2015. *Int J Environ Res Public Health* 2021, 18 (15), 7884. 10.3390/ijerph18157884. [PubMed: 34360177]
- (55). Park JH; Han YS; Ahn JS Comparison of Arsenic Co-Precipitation and Adsorption by Iron Minerals and the Mechanism of Arsenic Natural Attenuation in a Mine Stream. *Water Res* 2016, 106, 295–303. 10.1016/j.watres.2016.10.006. [PubMed: 27728822]
- (56). Chen G; Liu H Understanding the Reduction Kinetics of Aqueous Vanadium(V) and Transformation Products Using Rotating Ring-Disk Electrodes. *Environ Sci Technol* 2017, 51 (20), 11643–11651. 10.1021/acs.est.7b02021. [PubMed: 28902987]
- (57). Ramsay L; Petersen MM; Hansen B; Schullehner J; Van Der Wens P; Voutchkova D; Kristiansen SM Drinking Water Criteria for Arsenic in High-Income, Low-Dose Countries: The Effect of Legislation on Public Health. *Environ Sci Technol* 2021, 55 (6), 3483–3493. 10.1021/acs.est.0c03974. [PubMed: 33635640]

### Synopsis

A four-in-one vacuum-seal method was adapted into a material science technique to synthesize amorphous metal (hydr)oxides within the pore space of the most widely utilized point-of-use drinking filter systems to enable the co-removal of arsenic and other co-contaminants.

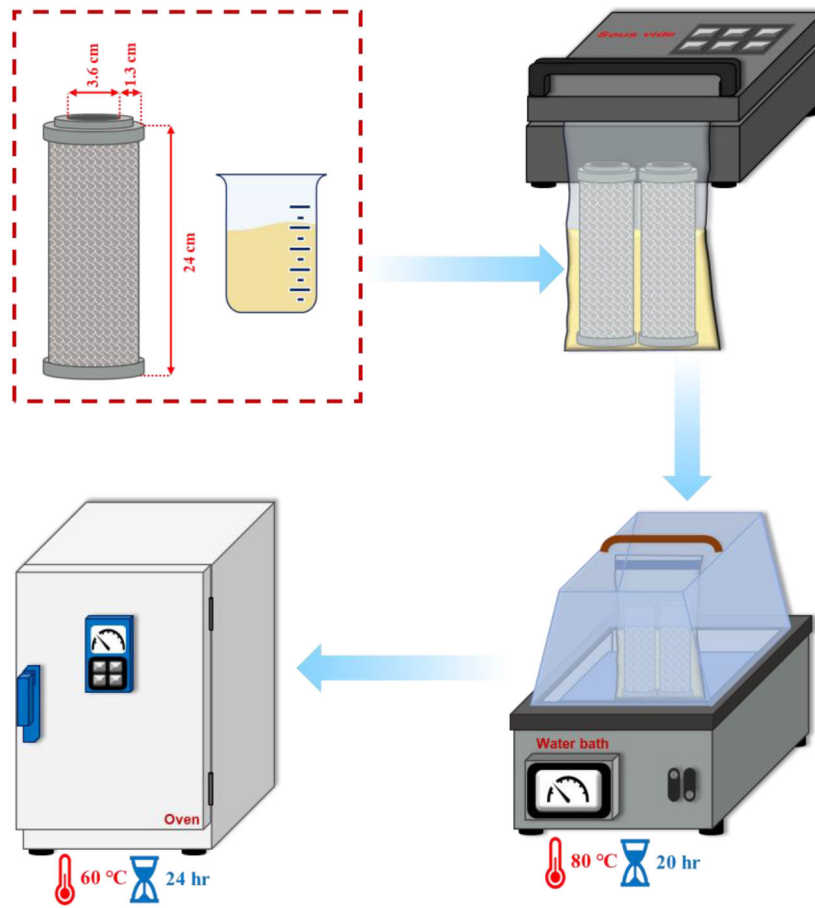


**Figure 1.** Carbon block dimensions and integrated four-in-one *Sous vide* impregnation procedure.



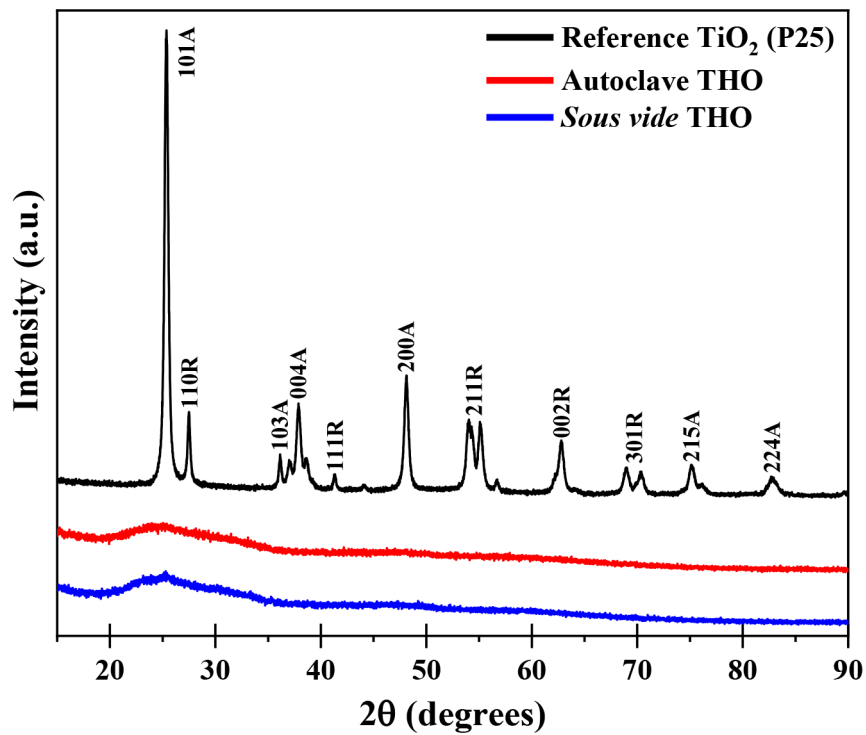


**Figure 2.** XRD spectra of the produced THO using *Sous vide* and conventional autoclave approaches compared with a reference  $\text{TiO}_2$ .

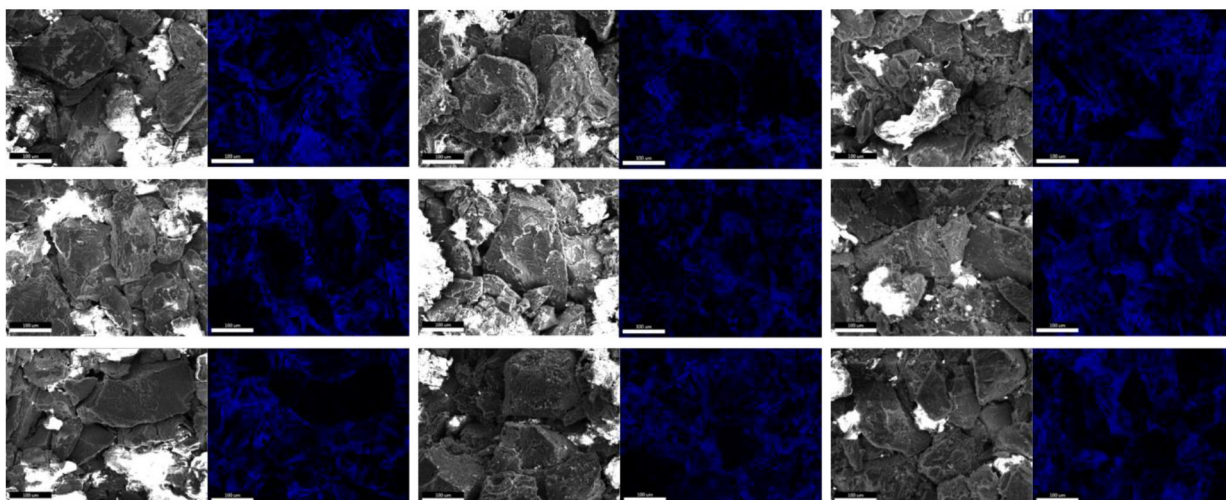


**Figure 3.**

Backscatter electron images and the correlated EDX Ti elemental mapping acquired from the bottom (left), middle (middle), and top (right) of the impregnated carbon block. Black and white images show the backscatter electron images acquired from the carbon block's cross-sections, and the blue spots show the Ti immobilized on the surface of the same cross-section as the acquired backscatter electron image.

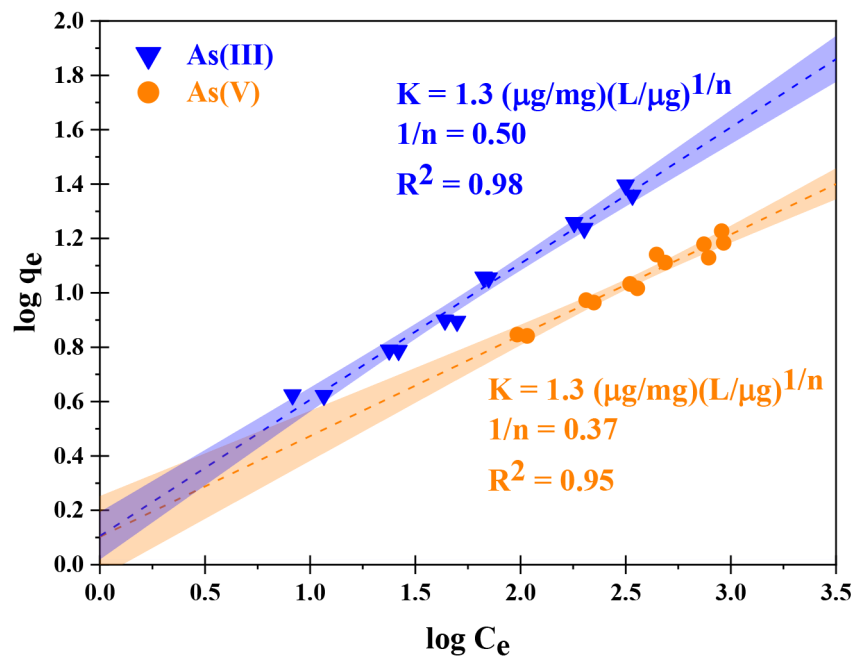


**Figure 4.** Linearized Freundlich isotherm fitting obtained from pseudo-equilibrium batch experiments results for arsenate and arsenite adsorption with amorphous THO. Experimental conditions:  $C_0(\text{As}) = 15 \mu\text{M}$  spiked in Tempe tap water, conductivity =  $1,368 \mu\text{S}/\text{cm}$ , pH = 7.9, and  $T = 23 \pm 1 \text{ }^\circ\text{C}$ .

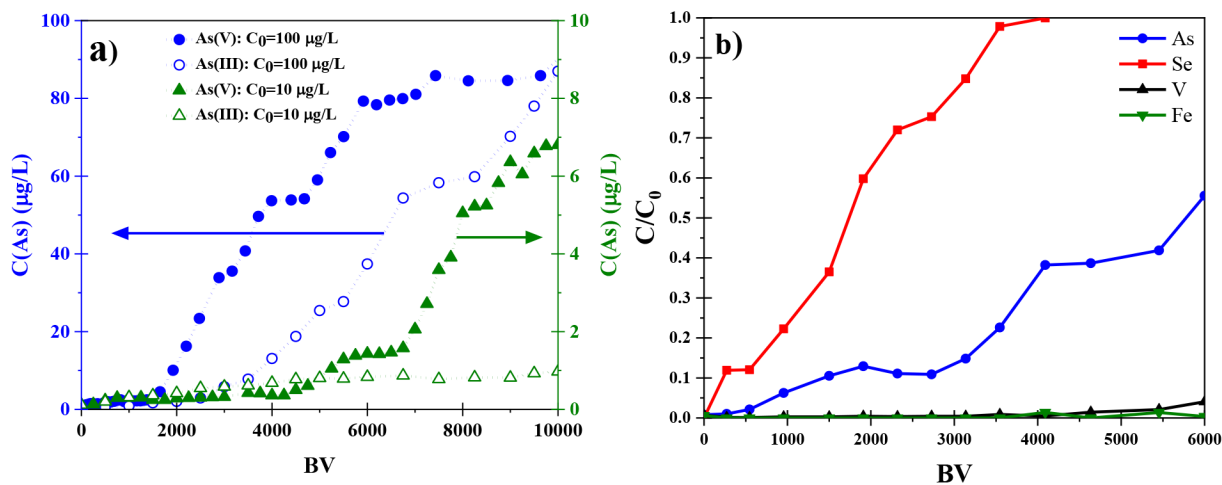


**Figure 5.**

Arsenate and arsenite breakthrough curves for THO-impregnated carbon block in Tempe tap water spiked with  $C_0(\text{As}) = 100 \mu\text{g/L}$  and  $C_0(\text{As}) = 10 \mu\text{g/L}$ , conductivity =  $1,368 \mu\text{S/cm}$  and  $\text{pH} = 7.9$ , EBCT = 0.48 min and  $T = 23 \pm 1 \text{ }^\circ\text{C}$  (a), and Se, V, Fe, and As breakthrough curves for THO-impregnated carbon block in actual groundwater with  $C_0(\text{As}) = 36 \mu\text{g/L}$ ,  $C_0(\text{V}) = 6 \mu\text{g/L}$ ,  $C_0(\text{Se}) = 9 \mu\text{g/L}$ ,  $C_0(\text{Fe}) = 7 \mu\text{g/L}$ , conductivity =  $1,132 \mu\text{S/cm}$  and  $\text{pH} = 8.2$ , EBCT = 0.48 min, and  $T = 23 \pm 1 \text{ }^\circ\text{C}$  (b).

**Table 1.**

Total chemicals consumption in each impregnation technique for different volumes of the carbon block

Impregnation method	Carbon block volume (cm <sup>3</sup> )	Total chemicals consumption (mL)
Conventional autoclave method	17	68.2
Conventional autoclave method with 2 full-size carbon blocks	960	3,887
The integrated method with 2 full-size carbon blocks	960	1,150

Author Manuscript

Author Manuscript

Author Manuscript

Author Manuscript